

## Electronic Tuning of Dynamical Charge Transfer at an Interface: K Doping of C<sub>60</sub>/Ag(111)

A. Peremans, Y. Caudano, and P. A. Thiry

*Laboratoire de Spectroscopie Moléculaire de Surface, Institute for Studies in Interface Sciences,  
Facultés Universitaires Notre-Dame de la Paix, 61 Rue de Bruxelles, B-5000 Namur, Belgium*

P. Dumas, W. Q. Zhang, A. Le Rille, and A. Tadjeddine

*Laboratoire pour l'Utilisation du Rayonnement Electromagnétique, Bâtiment 209D, F-91405 Orsay, France*

(Received 9 August 1996)

High-resolution vibrational spectroscopy of fullerene thin films is achieved by sum-frequency generation and infrared absorption. The  $A_g(2)$  mode of C<sub>60</sub> gains strong infrared activity when the molecule is adsorbed on Ag(111). K doping allows us to demonstrate the process of adsorbate/substrate dynamical charge transfer, by showing, for the first time, the quenching of the mode softening and infrared activity upon tuning of the admolecule electronic properties. These observations enable the quantitative evaluation of the coupling strength of the  $A_g(2)$  vibration to the  $t_{1u}$  orbital of C<sub>60</sub>. [S0031-9007(97)02811-1]

PACS numbers: 68.35.Ja, 63.20.Kr, 73.90.+f, 82.65.-i

Vibrational energy transfer at an interface is a fundamental process which controls the dynamics of surface reactions. Previous works, performed on small molecules such as CO interacting with ordered surfaces, point to the importance of the interfacial electronic structure in the process of vibrational energy dissipation [1]. Probing the influence of the admolecule electronic properties on the coupling of their vibrations to the substrate electrons appears necessary for assessing the proposed theoretical modeling. With that respect, we show that C<sub>60</sub> is an ideal probe molecule which enables the investigation of the electron-phonon coupling mechanisms operating at interfaces. The high symmetry of C<sub>60</sub> results indeed in a simplified electronic and vibrational structure [2,3]. Recent investigations further reveal a simple picture of the molecule chemisorption on metals where the lowest unoccupied molecular orbital (LUMO) of C<sub>60</sub> becomes partially filled upon hybridization with the electronic wave functions of the substrate [4–7]. However, probing the vibrational properties of fullerene thin films is hindered by the low infrared activity of the molecule, and vibrational spectroscopy of C<sub>60</sub> monolayers has been achieved only with low resolution (50 cm<sup>-1</sup>) using high-resolution electron-energy-loss spectroscopy (HREELS) [5–8] or, for corrugated surfaces, by Raman spectroscopy [9,10]. Hereafter, we show that sum frequency generation (SFG) in the midinfrared enables sensitive and high resolution (1.8 cm<sup>-1</sup>) vibrational spectroscopy of the C<sub>60</sub>/metal interface and that, according to an earlier attempt [11], conventional infrared absorption can detect the admolecule vibrations which have undergone a dramatic enhancement of their infrared activity via electron-phonon coupling. K doping of C<sub>60</sub> adsorbed on Ag(111) allows us to pinpoint the occurrence of dynamical charge transfer at the interface by showing, for the first time, the dependence of the latter process on the admolecule electronic structure. The present work also provides a first experimental evaluation

of an electron-phonon coupling strength in C<sub>60</sub> [12,13]. Finally, the improved resolution of this spectroscopic investigation allows us to refine the conclusions of previous works [5,6] regarding the inference of the adsorbed C<sub>60</sub> charge state from its vibrational fingerprint, a key physical quantity determining the layer electrical properties.

Following earlier works [11], we prepare the chemically polished Ag(111) single crystal in an ultrahigh vacuum environment by argon ion sputtering and subsequent annealing at 570 K. The C<sub>60</sub> epitaxial layer is obtained by saturating the Ag(111) surface with C<sub>60</sub> sublimated from a tantalum crucible while the substrate temperature is maintained at 570 K to prevent multilayer growth. Spectroscopic investigations and doping with potassium evaporated from a commercial getter source (SAES) are performed at 390 K. For SFG spectroscopy, we have developed a picosecond optical parametric oscillator (OPO) built around an AgGaS<sub>2</sub> crystal and synchronously pumped by a YAG laser. The OPO generates 11 ps long pulses, with linewidths of 1.8 cm<sup>-1</sup>, tunable from 2.5 μm (4000 cm<sup>-1</sup>) to 10 μm (1000 cm<sup>-1</sup>). The infrared beam (7 mW at 7 μm) is mixed at the interface with a visible beam (532 nm, ~30 mW, ~11 ps) obtained by frequency doubling 20% of the pump YAG laser beam. These beam characteristics allow us to achieve high-sensitivity SFG spectroscopy and to enlarge the applicability of SFG to the investigation of monolayers of macromolecules such as C<sub>60</sub>, the surface density of which is 1 order of magnitude lower than that of the highly packed monolayers usually studied by this nonlinear technique sensitive to the square of the admolecule surface density. The incidence angles of the two *p*-polarized beams are 65° and 55°, respectively. The photons coherently generated at the sum frequency are detected by a photomultiplier after spatial and spectral filtering. Infrared reflection-absorption spectroscopy is performed at grazing incidence with unpolarized light using a Fourier transform spectrometer (4 cm<sup>-1</sup> reso-

lution) equipped with a liquid nitrogen cooled mercury cadmium telluride detector.

Figures 1 and 2 show the evolution of the  $C_{60}/Ag(111)$  interface vibrational spectra upon K doping as measured by infrared and SFG spectroscopies, respectively. The clean  $Ag(111)$  sample at 570 K, prior to  $C_{60}$  deposition, is taken as a reference for the infrared data. The SFG spectra are untreated except for the normalization to the peak height of the highest frequency resonance labeled  $\alpha$ . Although the transfer of the sample for K doping excludes any accurate comparison of the SFG intensities between successive measurements, the observed intensity of the  $\alpha$  resonance is found to keep the same magnitude. Both spectroscopies show similar vibrational features: (1) The undoped  $C_{60}$  monolayer (curves *a* of Figs. 1 and 2) shows a single peak ( $\alpha$ ) at  $1445\text{ cm}^{-1}$  detectable by both spectroscopies. The correspondence of curve *a* in Fig. 1 with the infrared data obtained by Rudolf [11] testifies to the good quality of the sample. (2) K doping induces a weakening of the infrared activity and a softening of this  $\alpha$  mode (curves *a* to *b* in Figs. 1 and 2). (3) Both spectroscopies show an abrupt transition to a K-saturated phase (curves *c* in Figs. 1 and 2). This phase exhibits a new mode ( $\beta$ ) at  $1349\text{ cm}^{-1}$  detectable by both spectroscopies. Remarkably, the  $\alpha$  mode has completely lost its infrared activity but remains detected by SFG which enables the observation of the mode stiffening upon transition to the K-saturated phase (curves *b* to *c* in Fig. 2).

Electronic spectroscopies show the occurrence of charge transfer to  $C_{60}$  when adsorbed on  $Ag(111)$  [4] or on other metals [5]. The partial occupancy of the  $t_{1u}$  molecular orbital, the LUMO of the free molecule, further increases upon K doping to saturate to six electrons per molecule, corresponding to the complete filling of this sixfold-degenerated orbital. The potassium atoms, the coverage and adsorption site of which are not determined, act essentially as electron donors and the other perturba-

tions they induce on the molecular orbital and vibrational structures can be neglected to first approximation [4,5].

In accordance with these electronic properties, the vibrational characteristics of this K-saturated phase closely mimic those of  $C_{60}^{6-}$  such as in the  $K_6C_{60}$  bulk compound. Since the SFG cross section of a mode is proportional to the product of its infrared and Raman activities, comparing curves *c* in Figs. 1 and 2 shows that the  $\alpha$  ( $1430\text{ cm}^{-1}$ ) and  $\beta$  ( $1349\text{ cm}^{-1}$ ) modes are predominantly Raman and infrared active, respectively. They must be assigned to the Raman  $A_g(2)$  and infrared  $T_{1u}(4)$  modes located at  $1430\text{ cm}^{-1}$  [3] and  $1342\text{ cm}^{-1}$  [14,15] for  $C_{60}^{6-}$  in  $K_6C_{60}$ , respectively. The detection of the  $\beta$  mode in Figs. 1 and 2 results from a charged phonon effect which induces a dramatic enhancement of the  $T_{1u}(4)$  infrared band when the  $C_{60}$  molecule acquires a charge of six electrons, a process effective at the last stage of the doping leading to bulk  $K_6C_{60}$  [14,15]. The  $\beta$  peak position also confirms the six electron charge state since the  $7\text{ cm}^{-1}$  difference from the  $T_{1u}(4)$  mode frequency of  $C_{60}^{6-}$  in  $K_6C_{60}$  is negligible in front of the total charge induced mode softening of  $86\text{ cm}^{-1}$ . On the other hand, the SFG  $\alpha$  peak position of  $1430 \pm 0.5\text{ cm}^{-1}$  in curve *c* of Fig. 2 accurately obeys the correlation rule which relates the  $A_g(2)$  mode frequency ( $\gamma_{A_g(2)}$ ) to the  $C_{60}^{n-}$  charge state ( $n$ ) in bulk materials [3],

$$n = (1469\text{ cm}^{-1} - \gamma_{A_g(2)})/6.5\text{ cm}^{-1} \quad (1)$$

to give a charge state of  $6 \pm 0.1$  electrons.

Contrary to the K-saturated state, the vibrational characteristics of the undoped and moderately doped  $C_{60}$  layers (curves *a* to *b* in Figs. 1 and 2) cannot be related to known bulk phases of  $C_{60}$ . The  $\alpha$  mode frequencies do not correspond to any one of the four  $C_{60}$  infrared modes  $T_{1u}(1-4)$ , the infrared activities of which are indeed 2 orders of magnitude too small to give rise to the observed feature. The  $\alpha$  peak cannot result from the molecule deformation, since the breaking of the high molecular symmetry can make

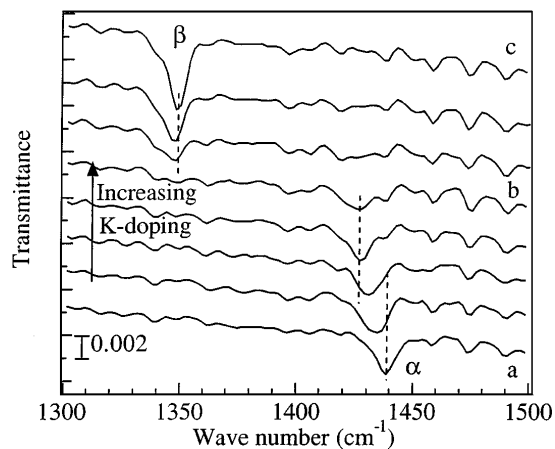


FIG. 1. K-doping evolved infrared spectra of  $C_{60}/Ag(111)$ . (a) Undoped, (b) K doped, and (c) K-saturated layer.

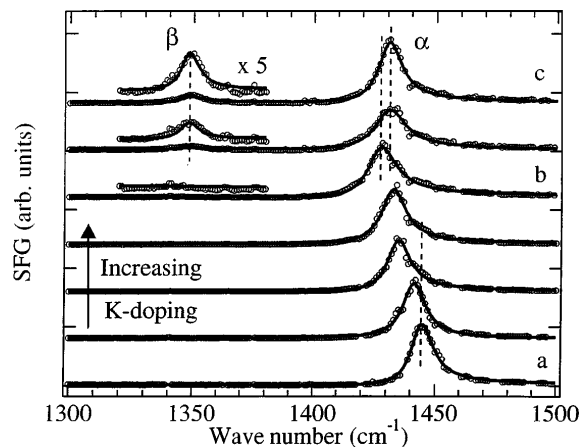


FIG. 2. As Fig. 1 but for SFG spectroscopy. The lines are fits to the SFG response of Lorentzian oscillators.

only the simple infrared fingerprint of  $C_{60}$  more complex with the appearance of additional bands of weaker intensity. Therefore a mode-specific electron-phonon coupling must account for the  $\alpha$  infrared band [1,16]. Indeed, we will demonstrate that this infrared feature stems from an interfacial dynamical charge transfer (IDCT). This particular electron-phonon coupling differs from the one leading to the observation of the  $\beta$  peak, by the fact that, in IDCT, the charge transfer is extramolecular.

IDCT has previously been invoked to account for the fast relaxation of the CO vibration and for the infrared activity of  $O_2$  [16] when these molecules are adsorbed on metals. As illustrated in Fig. 3, IDCT requires a vibration which modulates the energy ( $\varepsilon_a$ ) of a molecular orbital which is partially filled and hybridized with the substrate electronic wave functions. The vibration induces a charge oscillation between the substrate and the admolecule. The generated oscillating dipole is oriented perpendicular to the surface and can couple to an electromagnetic wave. Following a semiclassical description of this mechanism [1], we model the IDCT process by an oscillator driving force opposite to the electronic energy derivative versus the vibration normal coordinate,  $z$ . For a vibration interacting with one molecular orbital of energy  $\varepsilon_a$ , the motion equation reads

$$M\ddot{z} = -M\omega_0^2 z - \frac{\partial \varepsilon_a}{\partial z} n, \quad (2)$$

where  $M$ ,  $\omega_0$ ,  $\partial \varepsilon_a / \partial z$ , and  $n$  are the reduced mass and bare frequency of the vibration, the electron-phonon coupling strength, and the orbital occupancy, respectively. Neglecting the variation of  $n$  around its average value,  $\langle n \rangle$ , we find that the electron-phonon coupling induces essentially a shift of the oscillator equilibrium position:

$$\Delta z_0 = -\frac{\partial \varepsilon_a}{\partial z} \frac{\langle n \rangle}{M\omega_0^2}. \quad (3)$$

Because of the orbital hybridization with the continuum of the substrate wave functions, the modulation of  $\varepsilon_a$  induces indeed a slight oscillation of  $n$  which is proportional to the density of states of the orbital at the Fermi level,  $\rho_a(\varepsilon_f)$ :

$$n = \langle n \rangle - \rho_a(\varepsilon_f) d\varepsilon_a, \quad \text{with } d\varepsilon_a = \frac{\partial \varepsilon_a}{\partial z} z. \quad (4)$$

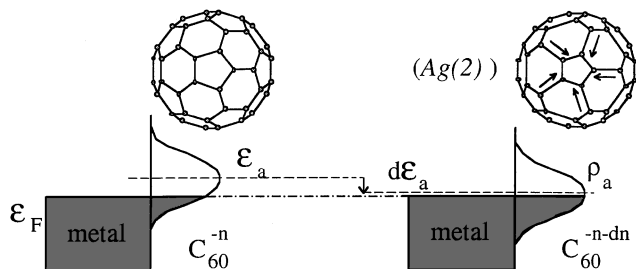


FIG. 3. The process of interfacial dynamical charge transfer.

This charge oscillation induces a mode softening from  $\omega_0$  to  $\Omega$ ,

$$\Omega^2 = \omega_0^2 - \frac{\rho_a(\varepsilon_f)}{M\%} \left( \frac{\partial \varepsilon_a}{\partial z} \right)^2, \quad (5)$$

and a dynamical dipole moment ( $\mu$  is the nondiagonal matrix element of the dipole moment operator),

$$\mu = e\rho_a(\varepsilon_f) \frac{\partial \varepsilon_a}{\partial z} d \sqrt{\frac{\hbar}{2M\Omega}}, \quad (6)$$

where  $d$  is the distance between the interface image plane and the charge centroid of the molecular orbital. The high symmetry of the  $C_{60}$  molecule gives stringent restrictions on the molecular vibrations that can be involved in a IDCT. No vibration modes other than the two  $A_g(1-2)$  singlets and the eight  $H_g(1-8)$  quintuplets can be coupled to the  $t_{1u}$  orbital [17] which is the only molecular orbital partially occupied before the saturation of the K doping is reached [4–6,9]. While the  $H_g(1-8)$  modes couple to quadrupolar density fluctuations, the two fully symmetric  $A_g(1-2)$  modes are allowed to modulate directly the  $t_{1u}$  orbital energy [17] and are expected to give rise to IDCT. These selection rules are consistent with the  $\alpha$  mode frequency in the moderately doped layers which corresponds to that of the “pentagonal pinch”  $A_g(2)$  mode (depicted in Fig. 3), the  $A_g(1)$  mode laying at a much lower frequency near  $500 \text{ cm}^{-1}$ .

Verifying the influence of the admolecule electronic properties on the infrared fingerprint is a necessary step towards the validation of the IDCT concept. K doping of  $C_{60}/\text{Ag}(111)/$  offers this opportunity. Since  $\rho_{t_{1u}}(\varepsilon_f)$  goes to 0 upon complete filling of the  $t_{1u}$  orbital, Eqs. (5) and (6) foresee the quenching of the softening and of the infrared activity of the  $A_g(2)$  mode at saturation of K doping. These effects are clearly observed in Figs. 1 and 2. The  $A_g(2)$  mode loses its infrared activity in curve  $b$  of Fig. 1. SFG spectroscopy enables the observation of the quenching of the mode softening which appears in Fig. 2 as a stiffening of the  $A_g(2)$  mode upon transition to the K-saturated phase.

The present work further allows a quantitative confirmation of the IDCT model. The dipole moment of the  $A_g(2)$  mode in  $C_{60}/\text{Ag}(111)$  is evaluated to  $\mu \approx 1 \cdot 10^{-1}$  Debye taking the surface density,  $M$ , and the Fresnel factor, equal to  $0.0115 \text{ \AA}^{-2}$  [18],  $2 \times 10^{-26} \text{ Kg}$ , and  $F^2/\cos(\theta) \approx 40$ , respectively. At the transition to the K-saturated state, the quenching of the mode softening is partially balanced by the frequency decrease which accompanies the last reduction step from  $C_{60}^{n-}$  to  $C_{60}^{6-}$ . Taking  $n$  between 5 and 6 and using Eqs. (5) and (6), the mode softening is evaluated to lay between 4 and  $10 \text{ cm}^{-1}$ . Such a softening can be deduced from the combination of Eqs. (5) and (6) if  $d$  and  $\rho_{t_{1u}}(\varepsilon_f)$  are adjusted in the expected range of  $\sim 1 \text{ \AA}$  and  $\sim 1$  state per eV, respectively. Knowing the last two parameters, the coupling strength of  $\partial \varepsilon_a / \partial z$  of

the order of  $\sim 0.6$  eV/Å is then deduced from Eq. (6). We note that a small value of  $d$  has already been invoked to account for the important contribution of the image potential to the  $t_{1u}$  shell electron affinity [7]. The relatively low density of states in comparison to the value of several states per eV inferred from electronic spectroscopies [5] suggests that only one out of the three spin-degenerated  $t_{1u}$  orbitals may be involved in the IDCT. The coupling strength inferred from the present work fits to theoretical estimates obtained by simple Keating or bond-charge model calculations [12,19]. Equation (4) suggests an alternative way to infer this value. Assuming that the electron-phonon coupling accounts for the pentagonal side contraction of  $2 \times 10^{-2}$  Å in  $C_{60}^{3-}$  measured, for example, for the  $Na_2CsC_{60}$  superconductor compound [13], we also obtain from Eq. (4) a value of  $\sim 0.7$  eV/Å for  $\partial \varepsilon_a / \partial z$ .

Regarding the inference of the  $C_{60}$  charge state, the present work underlines several surface-specific effects which hamper the extrapolation, from the bulk to the adsorbed phase, of the correlation rules, such as Eq. (1), which relate the  $C_{60}$  vibration frequencies to the molecule charge state. First, the  $A_g(2)$  mode softening induces an overestimation of the  $C_{60}$  charge state when using Eq. (1). This explains the inconsistencies that were observed when using these correlation rules for the two  $A_g(1-2)$  modes of  $C_{60}$ , measured by Raman spectroscopy, when the molecule was adsorbed on corrugated Au, Cu, and Ag [9]. Second, the frequencies of the  $T_{1u}$  vibrations in heavily charged  $C_{60}^{n-, n>4}$  can be affected, either by the metal screening and the dipole coupling because of the mode strong infrared activities, or by the hybridization of the  $t_{1u}$  orbital which perturbs the intermolecular electron-phonon coupling of the  $T_{1u}$  modes. These effects can account for the slight frequency mismatch ( $7$  cm $^{-1}$ ) between the  $T_{1u}(4)$  vibration of  $C_{60}^{6-}$  in the bulk and in the K-saturated adsorbed phases. However, the perfect correspondence of the  $A_g(2)$  mode frequency of the K-saturated phase with the prediction of Eq. (1) allows us to refine earlier conclusions [5,6] by showing that, in the absence of the effects mentioned above, the high frequency modes are accurate monitors of the molecule charge state.

In summary, the high-resolution vibrational study of  $C_{60}$  monolayers adsorbed on Ag(111) by SFG and infrared absorption spectroscopies allows us to pinpoint the coupling of the  $C_{60}$   $A_g(2)$  vibration to the substrate electrons via IDCT. In particular, this approach provides the first observations of the induced mode softening, as well

as the dependence of the coupling on the admolecule electronic structure. These observations validate the model of IDCT. The intramolecular coupling strength of the  $A_g(2)$  mode to the  $t_{1u}$  electrons is evaluated. This coupling can contribute either directly to the overall electron-phonon coupling responsible for superconductivity [12] or indirectly via the molecular deformation induced by the charge in  $C_{60}^{3-}$  [13].

It is a pleasure to thank Ph. Lambin, J.-M. Gilles, J. Darville, P. Rudolf, M. Tanguy, and P. Montel for fruitful discussions and/or efficient technical support. We acknowledge L.H. Tjeng *et al.* for providing us with Ref. [4] prior to publication. A.P. is a senior research associate of the National Fund for Scientific Research (Belgium) and Y.C. is holder of a grant of the Fund for Research in the Industry and Agriculture (Belgium). This work was supported by the Interuniversity Research Project on "reduced dimensionality systems" initiated by the Belgian Office for Scientific Technical and Cultural Affairs.

- 
- [1] D.C. Langreth and M. Persson, in *Laser Spectroscopy and Photo-Chemistry on Metal Surfaces*, edited by H.L. Dai and W. Ho, Advanced Series in Physical Chemistry Vol. 5 (World Scientific, Singapore, 1995), p. 498, and references therein.
  - [2] H. Kuzmany, R. Winkler, and T. Pichler, *J. Phys. Condens. Matter* **7**, 6601 (1995).
  - [3] S.J. Duclos *et al.*, *Science* **254**, 1625 (1991).
  - [4] L.H. Tjeng *et al.* (private communication).
  - [5] S. Modesti *et al.*, *Phys. Rev. Lett.* **71**, 2469 (1993).
  - [6] M.R.C. Hunt *et al.*, *Phys. Rev. B* **51**, 10 039 (1995).
  - [7] A.J. Maxwell *et al.*, *Phys. Rev. B* **49**, 10 717 (1994).
  - [8] G. Gensterblum *et al.*, *Phys. Rev. Lett.* **67**, 2171 (1991).
  - [9] S.J. Chase *et al.*, *Phys. Rev. B* **46**, 7873 (1992).
  - [10] A. Rosenberg *et al.*, *Chem. Phys. Lett.* **223**, 74 (1994).
  - [11] P. Rudolf, Ph.D. thesis, Univ. of Namur, Belgium, 1995.
  - [12] M. Schluter *et al.*, *Phys. Rev. Lett.* **68**, 526 (1992).
  - [13] K. Prassides *et al.*, *Science* **263**, 951 (1994).
  - [14] K.J. Fu *et al.*, *Phys. Rev. B* **46**, 1937 (1992).
  - [15] M.J. Rice and H.-Y. Choi, *Phys. Rev. B* **45**, 10 173 (1992).
  - [16] B.N.J. Persson, *Chem. Phys. Lett.* **139**, 457 (1987).
  - [17] M.S. Deshande *et al.*, *Phys. Rev. B* **50**, 6993 (1994).
  - [18] E.I. Altman and R.J. Colton, *Phys. Rev. B* **48**, 18 244 (1993).
  - [19] C.M. Varma, J. Zaanen, and K. Raghavashari, *Science* **254**, 989 (1991).